RSC Advances

ROYAL SOCIETY OF CHEMISTRY

www.rsc.org/advances

Cite this: DOI: 10.1039/c0xx00000x

www.rsc.org/xxxxxx

Communication

Biosynthesis approach of nitrogen doped graphene by denitrifying bacteria CFMI-1

Chunlin Zhu,[a] Zhangqi Feng,[a] Mengmeng Fan,[a] Chuntao Chen,[a] Bo Ma,[a,b] Jiazhi Yang[a] and Dongping Sun[*a]

Received (in XXX, XXX) Xth XXXXXXXXX 20XX, Accepted Xth XXXXXXXXX 20XX
DOI: 10.1039/b000000x

Here we present a novel approach to prepare N-doped graphene under ambient conditions by denitrifying bacteria CFMI-1. N element can be effectively introduced onto graphene and 8.2% (atom %) N doping level can be achieved. N-doped graphene possess size around 300-600 nm and an average thickness of 1-2 nm.

Recently, there were many methods for preparing N-doped graphene, such as chemical vapor deposition (CVD)[1], arc discharge of graphite electrodes in the presence of nitrogen atmosphere[2], thermal annealing graphene oxide (GO) with ammonia[3] or melamine[4], hydrothermal reduction of GO in the presence of hydrazine[5] and so on. Although above methods can prepare excellent N-doped graphene, they have some shortcomings in large scale production, such as toxic reagents, production cost, energy consumption, environmental concern.[6, 7] Thus, it is meaningful to explore a natural, mild and green method for introduction of nitrogen into graphene. As far as we are aware, however, the possibility for nitrogen-containing graphene sheets during the process of green reduction of GO has not been reported or exploited.

Here, a straight-forward and environment-friendly biosynthesis strategy was developed to fabricate N-doped graphene using denitrifying bacteria CFMI-1 as the reducing and N-doping bacteria. Denitrifying bacteria is an indispensable bacteria which can reduce inorganic nitrogen and carbon with high valence state.[8-10] Denitrifying bacteria have been found in a wide variety of environments, including soil, river and lake.[11,12] These microbes may have the ability to biosynthesis N-doped graphene. We use GO as a starting material to investigate the mild nitrogen doped reaction during the green reduction process. We investigate the N-doping and green reduction effect of GO by X-ray photoelectron spectroscopy (XPS) and energy dispersive X-ray detector (EDX). We explored the mechanism of GO-to-N-doped graphene with different components from denitrifying bacteria. Our research suggests that it is possible to synthesis N-doped graphene *via* green chemistry. Compared to non-environmental methods,[1-5] biosynthesis approach is simple, scalable, mild and environmentally friendly. The process of biosynthesis N-doped graphene does not involve toxic regents, complex processes, and high energy consumption. Thus, it is a low production cost, low energy consumption and high nitrogen doping level method. This capability also provides an opportunity for further investigation into the other biosynthesis N-doped graphene method.

The nitrogen doping of graphene greatly broadens its applications. For its satisfactory catalytic and electrochemical performances, N-graphene can be used in batteries, ultracapacitors.[13-15] More importantly, N doped graphene possess excellent biological properties including hemocompatibility, nontoxicity and water-dispersity.[16-18] Thus, it has been proposed as promising biomaterials, like biosensor,[19,20] drug carriers,[21] etc.

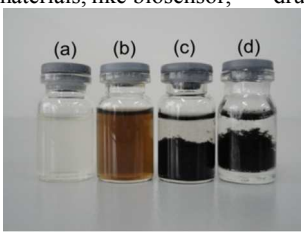

Figure 1. Microbial reduction of GO and biosynthesis of N-graphene occurred under anaerobic conditions. (Serum bottles a=pure denitrifying bacteria in the denitrifying medium without GO; b=blank control without bacteria; c=denitrifying bacteria microbial-reduced graphene (DNMG)-1 with bacteria after 3 days; d=DNMG-2 with bacteria after 5 days.)

Nitrogen doped graphene sheets were biosynthesized during the process of green reduction of graphene oxide by denitrifying bacteria CFMI-1 under anaerobic conditions. The reduction of GO to graphene was indicated by the gradual color change of the mixed culture solution. As shown in Figure 1, the deep yellow GO solution turned black within 2 days (Figure 1(c), DNMG-1), which suggested that graphene oxide be reduced to graphene with denitrifying bacteria CFMI-1. By comparison, no color change was observed in control experiment with denitrifying medium only (Figure 1(b)). Additionally, the suspension of the miscible

liquids turned clear after 5 days (Figure 1(d), DNMG-2). This phenomenon suggested that most of denitrifying bacteria sank to the bottom of the serum bottle.

As displayed in Figure S-1(a), the G and D bands are assigned to the graphitized structure and local defects/disorders, particularly N-graphene.[1] Moreover, the smaller ratio of I_D/I_G peak intensity it is, the lower defects/disorders we get in the structure.[22, 23] As shown in Figure S-1(a), the ratio of I_D/I_G of DNMG-1 (1.58) and DNMG-2 (1.44) is higher than that of CGO (graphene oxide prepared *via* chemical method) (1.40) and lower than that of CG (chemical reduced graphene) (1.72), indicating that the level of oxidation of DNMG is decreasing and the defects/disorders are increasing. This can be attributed to the formation of further sp^2 bonds in the sheets and appearance of vicious structure such as bong-angle and edge defects.[22, 27] Furthermore, the in-plane crystallite sizes La was inversely proportional to the intensity ratio of the D and G bands (I_D/I_G).[24] Thus, the crystallite size of DNMG decreases with the biosynthesis of N-graphene. In Figure S-1(b), the wave number of G-peak of DNMG shifts from 1589 cm^{-1} to 1578 cm^{-1} and 1576 cm^{-1} (apparent red shift), suggesting the transition from CGO to N doped graphene as mediated by denitrifying bacteria CFMI-1. The 2D peaks of DNMG appear at around 2685 cm^{-1}. Compared with the spectrum of single-layer graphene, the N-doped graphene exhibit a broader and up-shifted peak in the Raman spectra, indicating formation of multi-layer N-doped graphene sheets.[24] However, the intensity of 2D peaks of DNMG is very low, which may be caused by stacking of small sheets of DNMG in the process of reaction. The shape of 2D peak is symmetric, indicating weak inter-layer coupling exists between graphene layers and such coupling has been previously reported for graphene films grown *via* CVD.[25]

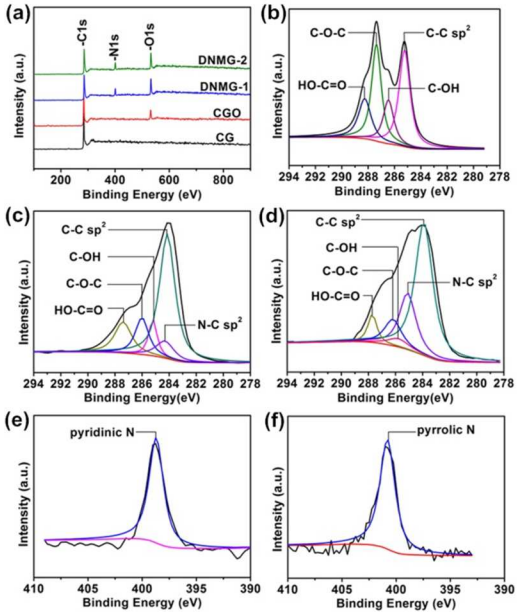

Figure 2. XPS spectra of (a) CG, CGO and DNMG, (b) C1s peaks and their resolution results of CGO, (c) DNMG-1 and (d) DNMG-2, N1s peaks and their resolution results of (e) DNMG-1 and (f) DNMG-2.

In order to analyse the change of functional groups before and after reaction, fourier transform infrared (FTIR) spectra was performed onto samples. As shown in Figure S-2, there is a small shoulder at 1192 cm^{-1} (Figure S-2(b) and (c)) corresponding to C–N in-plane stretching,[26-28] which can be attributed to microbial introduction of nitrogen by denitrifying culture medium and is confirmed in the following experiments.

High resolution XPS and wide XPS spectra were achieved to investigate the composition and chemical states of DNMG, (Figure 2). Through survey XPS survey spectra (Figure 2(a)), in addition to carbon and oxygen peaks, there is an obvious peak of nitrogen which demonstrated that nitrogen was introduced into graphene successfully during the bio-reduction process by denitrifying bacteria CFMI-1. With the increase of reduction time, the nitrogen doping level of DNMG increased to 8.2% (atom %, Table S-1). As shown in Figure 2(c) and 2(d), the peaks centered at the binding energies of 284.1, 285.2, 286.2 and 287.1 eV were assigned to C–C and C=C bonds, C–OH, O-C-O, and O=C–OH functional groups respectively.[29, 30] The peak located at the binding energies of 284.5 (Figure 2(c))and 284.9 eV (Figure 2(d)) were both contributed to N-sp^2C bands.[31, 32] As shown in Table S-2, the ratio of $A_{C\text{-}OH}/A_{C\text{-}C}$, $A_{C\text{-}O\text{-}C}/A_{C\text{-}C}$ and $A_{O=C\text{-}OH}/A_{C\text{-}C}$ had an obvious decrease, while the ratio of $A_{C\text{-}N}/A_{C\text{-}C}$ increased, which indicated denitrifying bacteria CFMI-1 possessed a strong capacity of N-doped during the process of reduction of CGO.

As a large proportion of nitrogen element, the high resolution N(1s) peak in Figure 2(e) and 2(f) was deconvoluted in order to study the composition and chemical states of nitrogen. The nitrogen (399.1 eV, Figure 2(e)) was mainly in the form of pyridinic N while the nitrogen (400.8 eV, Figure 2(f)) was mainly in the form of pyrrolic N.[4] This phenomenon can be attributed to the reaction between epoxy group and organic nitrogen, as well as reduction of oxygen containing functional groups. Firstly, the epoxy group on the basal planes of CGO react with organic nitrogen (produced by denitrifying bacteria CFMI-1) resulting in the formation of pyridinic N in the early stage of reduction. Secondly, with the further reduction, sp^2 carbon character was restored resulting in the increase of pyrrolic N. The increase of sp^2 nitrogen can be affirmed in FT-IR analysis (Figure S-2).

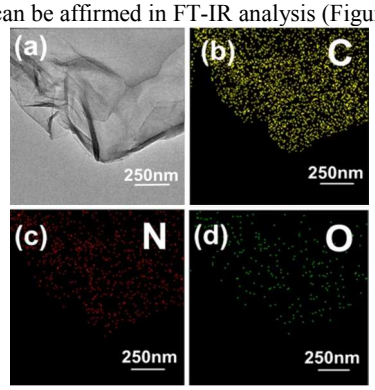

Figure 3. EDX analysis of DNMG-1, TEM image (a) and mapping of C (b), mapping of N (c) and mapping of O (d).

In order to further exhibit sheet structure and observe the content and distribution of N and O, FE-TEM image and EDX analysis (Figure 3) were conducted. As shown in Figure 3(a), the N-doped graphene appears to be in thin layers. The images of Figure 3(c) indicate that the whole basal plane of DNMG sheets contained a large amount of N with a uniform distribution density, evident of a facile N-doped reaction during the bio-reduction process. The EDX spectrum (Figure S-3) also can be affirmed that the content of N is considerable.

The representative TEM, AFM and FESEM images of as-obtained DNMG are displayed in Figure 4 and Figure S-4. It can be seen from Figure 4(a) and (b) that a few layers of graphene sheets were wrinkled and overlapped. Many more thin layers of graphene sheets appear around the edge parts, as shown in Figure 4(a). Figure 4(c) and (d) display the typical AFM image of DNMG after coating on a freshly cleaved mica substrate by spin-coating of their ethanol solution. The average size of the DNMG sheets varies widely between the nanometer to micrometer scale. The thickness of the graphene sheets are measured to be 1.62 nm and 3.46 nm from the height profile of the AFM image in Figure 4(e). A few small nano sheets are found in Figure 4(c), (d) and (e). These nano sheets are also proved to be graphene, with the size ranging from 300-600 nm and the height from 1-2 nm, which was probably resulted from the microbial reduction by denitrifying bacteria CFMI-1. These small size of DNMG consistent with those of FESEM images (Figure S-4) may cause mechanical defects to a certain extent. As shown in Figure S-4(a) and (c), the surface morphology of CG shows nubbly and heterogeneous distribution but uniform continuous structure for that of DNMG-1, suggesting that the size of reduced N-graphene by denitrifying bacteria is more uniform than that of CG. Most of surfaces are flat for DNMG, indicating that the stacking layers were significantly reduced which is confirmed in the Figure S-4(d).

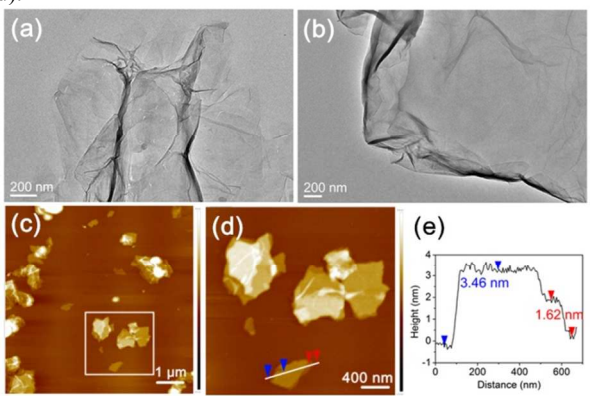

Figure 4. TEM images of DNMG after incubation of the GO (a and b). AFM images and cross-section height profile of DNMG (c-e).

The presence of an anodic peak and cathodic peak in the CV curves indicates that typical redox reaction occurred at the electrode surface. As shown in Figure S-5, the peaks of CG and DNMG are obviously higher than that of CGO, which is contributed to the reduction of oxygen functional groups. Due to their high surface charge, the ferricyanide ions are repelled at the electrode surface thereby limiting electrochemical reactions leading to a lower peaks. The peak separation potential of DNMG (ΔE_p = 0.70V) is close to that of CG (ΔE_p = 0.77V), indicating that DNMG possessed similar electrochemical properties.

So far, many green reducing agents and environment-friendly methods for reduction of GO have been developed to prepare graphene nanosheets (Table S-3), such as vitamin C,[33] polyphenols of green tea,[34] sugar,[35] glucose,[36] DMF reduction,[37] and solvothermal reduction[38]. In 2010, Tour's group[39] was the first to report that the bacteria *Shewanella* could easily reduce graphene oxide to graphene. Subsequently, *Eschericchia coli*[40] also has been demonstrated to reduce GO. However, simultaneous nitrogen doping and green reduction of graphene oxide has not been found in the above studies. In the study, N-doped graphene was prepared using denitrifying bacteria CFMI-1 as the N-doping bacteria. Herein, we propose the formation mechanism of N-doped graphene during the bio-reduction process of GO by denitrifying bacteria CFMI-1 (Figure S-6). As shown in Figure S-6 and Figure S-7, it is some or many substances secreted by denitrifying bacteria play a major role in preparing N-doped graphene. According to reduction graphene oxide by *Shewanella*,[39] extracellular cytochromes accelerated extracellular electron transfer between cells and graphene oxide. We inferred that extracellular cytochromes may be the major redox. The nitrogen source for doping is possible from NO_3^- in culture medium or nitrogenous compounds converted by microbial metabolism of denitrifying bacteria. The reduction effect of different components on CGO was shown in Figure S-7. The samples with spent medium (Figure S-7(b) and 7(c), a 100-mL 24-h denitrifying bacteria growth culture was filtered through a 0.22 μm filter.) The clear light yellow filtrate was called spent medium, which slowly turned black within 5 days, in contrast to the medium control (Figure S-7(a)) and the pure cells control (Figure S-7(c) and 7(d)), demonstrating the formation of suspended graphene. This results clearly suggested that redox active compounds, e.g., electron shuttle(s) or extracellular cytochromes were secreted by denitrifying bacteria CFMI-1.[8-10] The redox active compounds can accelerate the rate of electron transfer. Although the above results were consistent with those by *Shewanella*,[39] a striking difference was that the former had faster rate of reduction. Therefore, it is affirmed that denitrifying bacteria CFMI-1 can produce and excrete substantial redox active compounds which play an important role in reducing GO. In order to clearly reveal the bio-reduction and N-doped mechanisms, further studies should be concentrated on the exploration of extracellular electron transfer pathways and electron mediators for the N-doped biosynthesis process by denitrifying bacteria CFMI-1.

In summary, N element was successfully introduced onto the graphene during the bio-reduction of graphene oxide by denitrifying bacteria CFMI-1. The atomic percentage of nitrogen in doped graphene samples can be adjusted up to 8.2%. The study on denitrifying bacteria CFMI-1 reduction not only discovers a new environmental friendly microorganism for preparation of N-doped graphene in large-scale production, but also provides a reference for systematic study of microbial preparation of green materials. The yield of N-doped graphene by denitrifying bacteria CFMI-1 can continue to be improved and the suitable conditions of microbial reduction of GO need further studies.

This work was supported by "National Natural Science Foundation of China (No. 51272106) ", "Research Fund for the Doctoral Program of Higher Education of China (RFDP) (No.20123219110015)", "The Fundamental Research Funds for the Central Universities (No. 30920130121001)" and "A Project Funded by the Priority Academic Program Development of Jiangsu Higher Education Institutions (PAPD, China)".

Notes and references

[a] *Chemicobiology and Functional Materials Institute of Nanjing University of Science and Technology, Xiao Ling Wei 200, Nanjing,*

210094, China. Fax: 86-25-84431939; Tel: 86-25-8431579; E-mail: sundpe301@163.com
[b] *Department of Life Sciences of Lianyungang Teacher's College, Sheng Hu Lu 28, Lianyungang, 222006, China.*

† Electronic Supplementary Information (ESI) available: [Expeimental section, Raman spectra, FTIR, FE-SEM images and cyclic voltammetry of DNMG, proposed mechanism of biosynthesis of N-doped graphene, photo of CGO suspensions at different time using spent medium and cells only, table of nitrogen atomic percent, ratios of the oxygen and nitrogen-containing bonds to the C-C bonds for samples.]. See DOI: 10.1039/b000000x/

1. D. Wei, Y. Liu, Y. Wang, H. Zhang, L. Huang and G. Yu, *Nano Letters*, 2009, **9**, 1752–1758.
2. L. Guan, L. Cui, K. Lin, Y. Wang, T. Wang, M. Jin, F. He, X. Chen and S. Cui, *Applied Physics A*, 2011, **102**, 289–294.
3. D. Geng, Y. Chen, G. Chen, Y. Li, R. Li, X. Sun, S. Ye and S. Knights, *Energy & Environmental Science*, 2011, **4**, 760–764.
4. B. Zheng, T. Chen, F. Xiao, W. Bao and X. Xia, *Journal of Solid State Electrochemistry*, 2013, **17**, 1809–1814.
5. X. Li, H. Wang, J. Robinson, H. Sanchez, G. Diankov and H. Dai, *Journal of the American Chemical Society*, 2009, **131**, 15939–15944.
6. Z. Jin, J. Yao, K. Carter and M. James, *ACS Nano*, 2011, **5**, 4112-4117.
7. Y. Wang, Y. Y. Shao, D. W. Matson, J. H. Li and Y. H. Lin, *ACS Nano*, 2010, **4**, 1790-1798.
8. L. Zhuang, Y. Yuan, G. Q. Yang and S. G. Zhou, *Electrochemistry Communications*, 2012, **21**, 69–72.
9. J. Trögl, O. Krhůtková, V. Pilařová, P. Dáňová, R. Holíček, M. Kohlová, S. Hejda, J. Smrčka, A. Boušková and L. Křiklavová, *Int. J. Environ. Sci. Technol.*, 2012, **9**, 425-432.
10. W. I. Ohtsubo, M. Miyahara, T. Yamada, A. Watanabe, S. Fushinobu, T. Wakagi, H. Shoun, K. Miyauchi and G. Endo, *Journal of Bioscience and Bioengineering*, 2013, **6**, 722-724.
11. H. S. Bae, W. T. Im, Y. C. Suwa, J. M. Lee and Y. K. Chang, *Arch. Microbiol.*, 2009, **191**, 329–340.
12. K. J. Chae, S. M. Kim, S. E. Oh, X. H. Ren, J. Lee and I. S. Kim, *Bioprocess Biosyst. Eng.*, 2012, **35**, 1157–1165.
13. N. Soin, S. S. Roy, S. Sharma, T. Thundat and J. A. McLaughlin, *J. Solid State Electr.*, 2013, **17**, 2139-2149.
14. D. Hulicova-Jurcakova, M. Kodama, S. Shiraishi, H. Hatori, Z. H. Zhu and G. Q. Lu, *Adv. Funct. Mater.,* 2009, **19**, 1800–1809.
15. A. Tiwari and S. K. Shukla, Advanced carbon materials and technology, *Wiley - Scrivener*, USA, 2014.
16. A. Tiwari and A. P. F. Turner, Biosensors Nanotechnology, *Wiley - Scrivener*, USA, 2014.
17. J. Tyagi and R. Kakkar. *Advanced Materials Letters*, 2013, **4**, 721-736.
18. M. X. Guo, M. Li, X. Q. Liu, M. L. Zhao, D. J. Li, D. S. Geng, X. L. Sun and H. Q. Gu, *J. Mater. Sci. Mater. Med.,* 2013, **24**, 2741-2748.
19. O. Parlak, A. Tiwari, A. P. F. Turner and A. Tiwari. *Biosensors and Bioelectronics*, 2013, **49**, 53-62.
20. O. Parlak, A. P. F. Turner and A. Tiwari. *Advanced Materials*, 2014, **26**, 482-486.
21. S. K. Singh, M. K. Singh, P. P. Kulkarni, V. K. Sonkar, J. J. A. Gracio and D. Dash, *ACS Nano,* 2012, **6**, 2731-2740.
22. M. Hayatsu, K. Tago and M. Saito, *Soil Sci. Plant. Nutr.*, 2008, **54**, 33–45.
23. W. S. Hummers and R. E. J. Offeman, *Am. Chem. Soc.*, 1958, **80**, 1339.
24. S. Ryu, M. Y. Han, J. Maultzsch, T. F. Heinz, P. Kim, M. L. Steigerwald and L. E. Brus, *Nano Lett.*, 2008, **8**, 36–41.
25. H. Wang, T. Maiyalagan and X. Wang, *ACS Catal.*, 2012, **2**, 781−794.
26. D. Yang, A. Velamakanni, G. Bozoklu, S. Park, M. Stoller, R. D Piner, S. Stankovich, I. Jung, D. A. Field, C. A. Ventrice Jr and R. S. Ruoff, *Carbon*, 2009, **47**, 145–152.
27. D. R. Lenski and M. S. Fuhrer, *J. Appl. Phys.*, 2011, **110**, 013720.
28. K. Krishnamoorthy, M. Veerapandian, K. Yun and S. J. Kim, *Carbon*, 2013, **53**, 38–49.
29. H. L. Guo, X. F. Wang, Q. Y. Qian, F. B. Wang and X. H. Xia, *ACS Nano*, 2009, **3**, 2653-2659.
30. A. C. Ferrari and J. Robertson, *Phys. Rev. B.*, 2000, **61**, 14095–14107.
31. J. C. Meyer, A. K. Geim, M. I. Katsnelson, K. S. Novoselov, T. J. Booth and S. Roth, *Nature*, 2007, **446**, 60-63.
32. D. Motlagh, J. Yang, K. Y. Lui and A. R. Webb, *Biomaterials*, 2006, **27**, 4315-4324.
33. M. J. Fernández-Merino, L. Guardia, J. I. Paredes, S. Villar-Rodil, P. Solís-Fernández, A. Martínez-Alonso and J. M. D. Tascón, *J. Phys. Chem. C*, 2010, **114**, 6426–6432.
34. O. Akhavan, M. Kalaee, S. Z. Alavi, S. M. A. Ghiasi and A. Esfandiar, *Carbon*, 2012, **50**, 3015-3025.
35. C. Zhu, S. Guo, Y. Fang and S. Dong, *ACS Nano*, 2010, **4**, 2429-2437.
36. O. Akhavan, E. Ghaderi, S. Aghayee, Y. Fereydooni and A. Talebi, *J. Mater. Chem.*, 2012, **22**, 13773-13781.
37. K. Ai, Y. Liu, L. Lu, X. Cheng and L. Huo, *J. Mater. Chem.*, 2011, **21**, 3365-3370.
38. O. Akhavan, M. Choobtashani and E. Ghaderi, *J. Phys. Chem. C*, 2012, **116**, 9653-9659.
39. E. C. Salas, Z. Sun, A. Lüttge and J. M. Tour, *ACS Nano*, 2010, **8**, 4852-4856.
40. O. Akhavan and E. Ghaderi, *Carbon*, 2012, **50**, 1853-1860.